Iranian Journal of Medical Physics

ijmp.mums.ac.ir

IJMP

A Feasibility Study to Reduce the Contamination of Photoneutrons and Photons in Organs/Tissues during Radiotherapy

Roya Boodaghi Malidarre [1], Rahim Khabaz [2*], Mohammad Reza Benam [1], Vahid Zanganeh [2]

1. Department of Physics, Payame Noor University (PNU), Tehran, Iran
2. Department of Physics, Faculty of Sciences, Golestan University,Gorgan, Iran

ARTICLE INFO

Article type:
Original Paper

Article history:
Received: Jun 03, 2019
Accepted: Dec 13, 2019

Keywords:
Linac
Radiations
Shielding
Absorbed dose

ABSTRACT

Introduction: Due to out-of-field effects in radiation therapy, the determination and reduction of both unwanted photon and photoneutron doses are essential for the reasonable assessment of the risks to healthy tissues.

Material and Methods: By the application of a multilayer shield throughout the phantom and using two models for photoneutron and photon sources, doses were estimated in a 15-MV linac in tissues and organs. Different neutron moderators were used, and the best materials, such as polyethylene, polystyrene, polyvinyl chloride, paraffin, and water, were reported for shielding purpose. Boron carbide and steel were utilized as neutron and gamma absorbents. Various lengths of the shield in line with phantom stature were also assessed in this study.

Results: Except for the target organ, with the shield throughout the phantom, both photoneutron and photon doses approximately reduced by 57-89% and 88-95%, respectively. Extra photoneutron dose in the photon source was also reported due to the shield. Then, unwanted doses, especially photon dose remarkably decreased with increasing the steel thickness. The smaller dimensions of the shield caused also a considerable reduction of the photoneutron and photon doses in the phantom.

Conclusion: The application of a multilayer shield reduces the photon dose remarkably in healthy tissues. Therefore, it is recommended to use shielding materials to decrease photoneutron and photon doses, which can cause a reduction in the risk of secondary cancer. Due to the relatively high mass of the shield, it is necessary to design a proper device to maintain and move the structure.

► *Please cite this article as:*
Boodagh Malidarre R, Khabaz R, Benam MR, Zanganeh V. A Feasibility Study to Reduce the Contamination of Photoneutrons and Photons in Organs/Tissues during Radiotherapy. Iran J Med Phys 2020; 17: 366-373. 10.22038/ijmp.2019.40879.1579.

Introduction

Cancer, as an uncontrolled growth of cells, often invades healthy tissues. Radiation therapy is adopted as an established way for cancer treatment due to maximizing the radiation dose to the tumor volume and minimizing the radiation dose to the healthy organs and tissues [1]. The most important concern in radiotherapy is secondary out-of-field radiation due to the high relative biological effectiveness (RBE) of photoneutron source [2-4]. In addition to photoneutron, photon source has also a significant contribution to secondary malignancies [5,6]. The production of photoneutrons occurs when high energy photons interact with the structures of the linear accelerator (linac) head [1, 5, 7, 8].

Since the information on the physical properties of photoneutron and photon is often necessary for the calculation of the doses in organs, both neutron source and photon models are required. We have been used simplified model for evaluation of dose in tissues and organs in the previous study [9]. In a previous study, a corrected simplified model was used since calculations were performed in the presence of phantom, head, and walls of the treatment room simultaneously [9]. In the corrected simplified model, a spherical tungsten shell was simulated with the neutron source term, which was placed in the center, and a cone aperture was considered in the shell to produce a 10×10 cm² radiation field at the isocenter [9,10].

In order to mitigate the discrepancy in the low energy region for the photoneutron spectrum, the Hf-In-Cd-Boral filters were used in the opening of the cone, and then, the photoneutron energy spectrum was represented in the corrected simplified model [9]. It was shown that the values of photoneutron equivalent average dose to organs and tissues due to high RBE are remarkable; therefore, it is essential to design a proper shield for the reduction of out-of-field doses.

To calculate photon effect on the organs, a point source of photons located in the head of the cone was also simulated in the presence of the treatment room

**Corresponding Author:* Tel & Fax: +98 01732245882; E-mail: r.khabaz@gu.ac.ir; ra_khabaz@yahoo.com

walls. The spatial distribution of photons was obtained by the application of the phase-space file in Geant4.10.5. In addition, the principle of as low as reasonably achievable (ALARA), which is the International Commission on Radiological Protection (ICRP) recommendation, was suggested for the protection of patients in the therapeutic treatment [11]. Therefore, different shielding slabs, including neutron moderator, neutron absorbent, and gamma absorbent, were applied throughout the phantom, and dose reduction rates of photoneutron and photon were evaluated in the present study.

Various kinds of materials were used for moderating photoneutrons, and the best materials were reported in this regard. The extra photoneutron dose due to photon source interaction with the shield was also calculated in the present study. Garrigo et al. used the lead shield in radiation therapy for the two cases with and without a shield in breast cancer [12].

Roy et al. investigated both scattered photon and photoneutron reduction by applying polyethylene and lead shield in the position of the fetus for breast cancer and understood that the lead shield diminishes scattered photoneutron and photon rates by 40% and 50%, respectively. By adding borated polyethylene as shield photoneutron, dose reduces by the factor 7.5 in contrast to unshielded value [13]. The aim of this study was the reduction of doses due to photons and photoneutrons to healthy tissues and organs of a patient with pelvic cancer submitted for radiotherapy treatment by choosing a proper shield.

Materials and Methods

Irradiation was performed for pelvic treatment, especially uterus for 0^0 gantry angles of the 15-MV linac. Photoneutron/photon transport Monte Carlo MCNPX code (version 2.6) was employed using the anthropomorphic revised form of Medical Internal Radiation Dose (MIRD) phantom with 175 cm height and 20 cm width. The walls of the treatment room in both sources were also modeled by concrete with a density of 2.35 (gr/cm^3) with elemental compositions of 0.6% Hydrogen (H), 50.0% Oxygen (O), 1.7% Sodium (Na), 4.8% Aluminium (Al), 31.5% Silicon (Si), 1.9% Potassium (K), 8.3% Calcium (Ca), and 1.2% Iron (Fe) (in terms of their weight percentage) [9].Since photoneutron and photon transport are needed for the calculation of the doses in organs or tissues using Monte Carlo, and direct measurements are not feasible, new models were represented for the evaluation of spectra and doses. The simplified model of the linac head as a tungsten hollow sphere with a thickness of 10 cm and a conical air-filled aperture were simulated according to the National Council on Radiation Protection and Measurements (NCRP) 79 [10]. As in a previous study [9], the four Hafnium-Indium-Cadmium-Boral filters under the cone were employed for photoneutron sources in order to mitigate the differences for the low-energy region in the photoneutron energy spectrum.

Since photon also contributes a significant unwanted out-of-field dose to the patient, the photon source term is sited in the head of a cone in another program. Photon beams were limited to irradiate in the region of the cone to investigate secondary photon doses. For having the 10×10 cm^2 radiation field, the half angle of the cone was considered 17^0 for uterus treatment.

Various types of shielding materials were used in order to reduce the secondary radiation doses to out-of-field of the photoneutron and neutron sources in radiation therapy. According to the ICRP principle of ALARA, the proper shielding materials were designed to decrease both photoneutron and photon doses to organs or tissues simultaneously to an acceptable level and produce less extra photoneutron dose due to photon interaction with the shield. A variety of hydro and carbon materials for moderating neutron with different thicknesses was applied for proper shielding structures, and the best materials were chosen and reported in this regard.

At first, shielding materials comprised of steel sheets with a total thickness of 5.0 cm on the bottom in combination with 2.5 cm thick boron carbide in the middle and 2.5 cm thick neutron moderator on the top of the phantom A hole was created on top of the target volume to permit the radiation received by the target organ. These cakes were repeated twice throughout the phantom. It means that they were constructed as a multilayer.

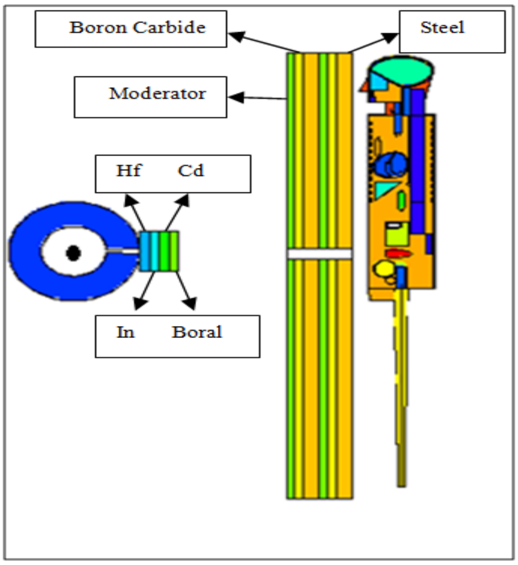

Figure 1. Schema of multilayer shield throughout phantom for neutron source

The dimension of these sheets was 20×20×4 cm^3. Boron carbide and steel were used as thermal-neutron and gamma absorbents, respectively. The reason for the application of boron carbide as a thermal-neutron absorbent in the shield is the main contribution of the thermal neutron to photoneutrons associated with 15-MV X-ray beams [13]. The total thicknesses of the multilayers of boron carbide, neutron moderator, and steel were selected as 20 cm.

Different materials were placed instead of neutron moderator the best of which were reported as polyethylene (C_2H_4) with a density of 0.94 g/cm^3, paraffin ($C_{25}H_{52}$) with a density of 0.93 g/cm^3, polystyrene (C_8H_8) with a density of 1.06 g/cm^3, polycarbonate ($C_{16}H_{14}O_3$) with a density of 1.20 g/cm^3, water (H_2O) with a density of 0.99 g/cm^3, and polyvinyl chloride (PVC) (C_2H_3Cl) with a density of 1.40 g/cm^3 [14]. The schema of photoneutron source model and phantom in the presence of a shield between them is presented in Figure 1.

Extra photoneutrons may be produced due to the presence of shielding structures and interaction between the photon source and shield. These interactions were considered by Phys card in MCNPX code for photon source, and then the doses were estimated. Following that, in order to represent the effect of steel thickness on photoneutron and photon doses, the steel thickness also varied to the values of 0.5, 2.5, and 5.0 cm in each multilayer cake, and the results were reported in this regard. Due to the high mass of the shield, the smaller dimensions of the shield were considered to investigate the reduction dose of photoneutron and photon. Therefore, the lengths of 40, 50, and 60 cm for the shield in line with phantom stature were chosen, and the results were reported in this regard.

Results

The photon energy spectrum at the isocenter is calculated and represented in Figure 2. The 2×10^9 histories were followed for the photon energy spectrum, and the maximum uncertainty was reported as 5%. Error bars are also shown in Figure 2.

Then, the values of the photoneutron dose received by organs and tissues in the absence and presence of the shield were calculated, and their comparison is depicted in Figure 3. The results of this comparison by the consideration of different neutron moderators are also illustrated in Figure 3.

The results of the comparison of absorbed dose in the absence and presence of the shield for different neutron moderators are illustrated in Figure 4.

Table 1 tabulates the reduction rates for photoneutron and photon in different neutron moderators as shields.

In addition, in order to show the honesty of the applied shielding materials, the values of extra photoneutron dose due to shielding structures by photon source were compared to photoneutron dose in neutron source. Therefore, one can be convinced that the extra photoneutron dose value is ignorable. Figure 5 depicts the photoneutron dose due to photon source interaction with the shield.

Then, for polyethylene moderator, steel thickness varied as 0.5, 2.5, and 5.0 cm. The photoneutron and photon absorbed doses in various organs and different steel thicknesses are shown in figures 6 and 7, respectively.

Table 2 tabulates the calculation results of the photoneutron and photon reduction rates for different lengths of the shielding materials.

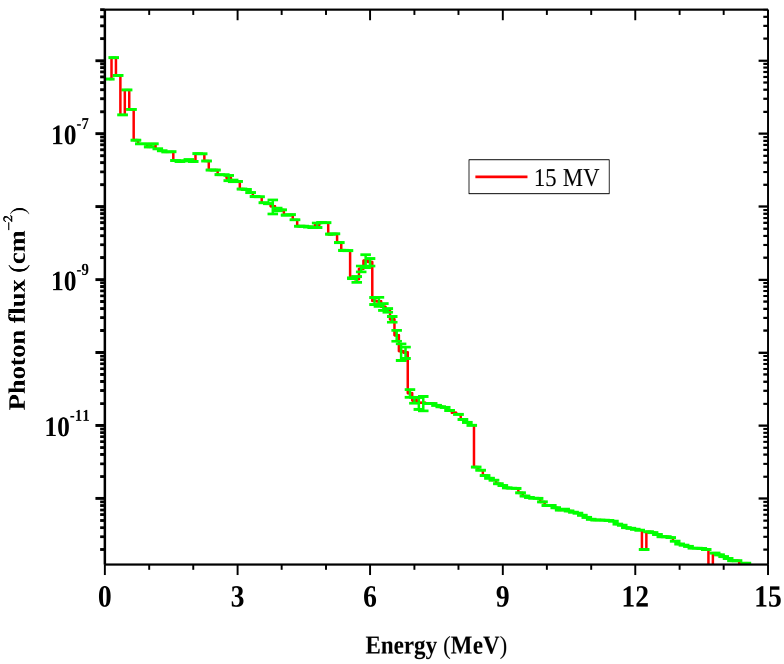

Figure 2. Photon energy spectrum at isocenter for 15-MV linac (Error bars are shown by green line)

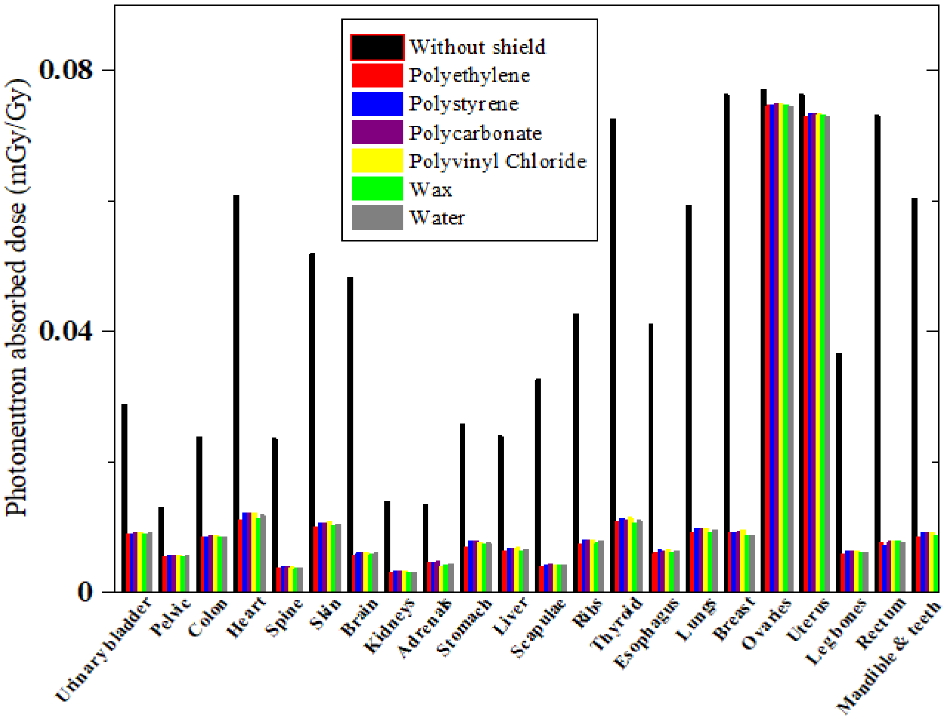

Figure 3. Comparison of photoneutron absorbed dose without shield and with different shielding materials in each tissue and organ for 15-MV linac (steel thickness: 5 cm)

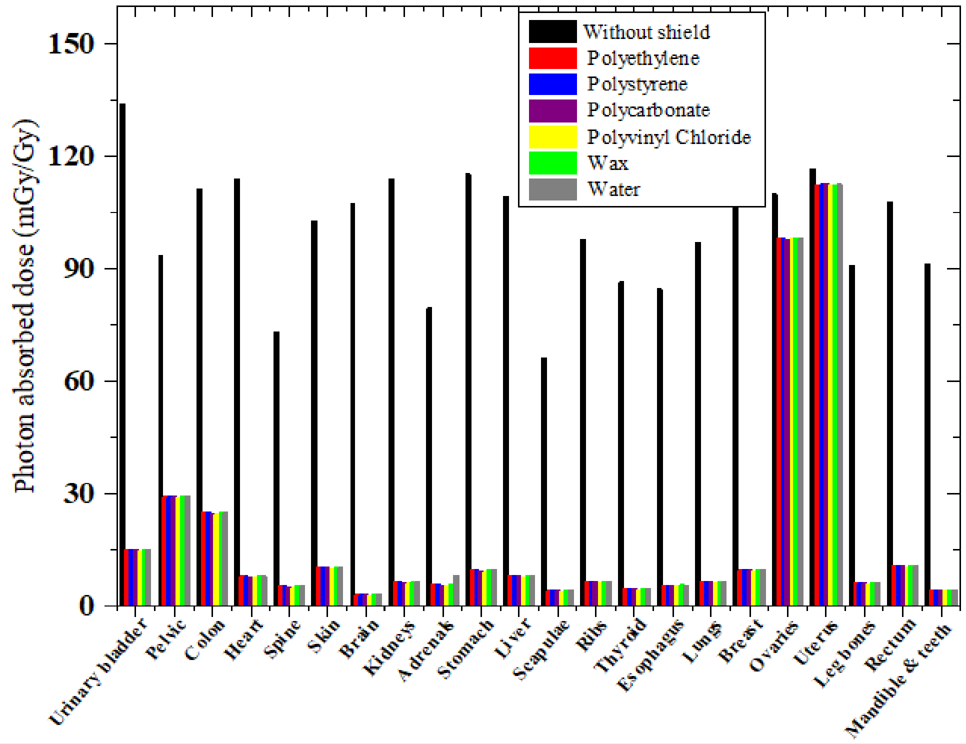

Figure 4. Comparison of photon absorbed dose without shield and with different shielding materials in each tissue and organ for 15-MV linac (steel thickness: 5 cm)

Table 1. Photoneutron and photon reduction rates for different neutron moderators in 15-MV linac

Organ	Polyethylene reduction (%)		Polystyrene reduction (%)		Polycarbonate reduction (%)		Polyvinyl chloridereduction (%)		Wax reduction (%)		Water reduction (%)	
	Neutron	Photon	Neutron	Photon	Neutron	Photon	Neutron	Photon	Neutron	Photon	Neutron	Photon
Urinary bladder	69.53	88.67	69.12	88.69	68.11	88.69	68.56	88.69	69.12	88.69	68.80	88.69
Pelvic	58.28	68.82	57.06	68.82	57.06	68.82	56.75	68.83	58.05	68.82	57.59	68.82
Colon	65.22	77.59	64.21	77.60	63.67	77.60	63.88	77.60	64.80	77.61	64.34	77.60
Heart	81.71	93.03	79.98	93.06	80.06	93.06	80.08	93.06	81.36	93.06	80.51	93.06
Spine	84.70	92.87	83.77	92.87	83.72	92.87	83.70	92.87	84.49	92.88	84.11	92.87
Skin	80.85	89.97	79.48	89.98	79.39	89.98	79.10	89.99	80.54	89.98	79.85	89.98
Brain	88.43	97.20	87.60	97.20	87.52	97.20	87.40	97.22	88.08	97.20	87.71	97.20
Kidneys	77.96	94.40	76.58	94.43	76.80	94.43	76.72	94.43	78.03	94.43	77.45	94.42
Adrenals	66.54	92.69	66.69	92.73	64.84	92.73	70.69	92.74	68.84	92.73	67.51	92.73
Stomach	72.78	91.70	70.07	91.70	69.92	91.70	70.42	91.70	71.85	91.71	71.08	91.70
Liver	73.85	92.59	71.85	92.60	71.76	92.60	71.60	92.62	73.48	92.60	72.56	92.60
Scapulae	87.85	93.59	87.11	93.58	87.05	93.58	87.08	93.59	87.63	93.57	87.20	93.58
Ribs	82.80	93.24	81.42	93.25	81.32	93.25	81.06	93.25	82.35	93.25	81.67	93.25
Thyroid	84.99	94.56	84.50	94.55	84.86	94.55	84.37	94.56	85.36	94.54	84.89	94.55
Esophagus	85.43	93.40	84.06	93.41	84.74	93.41	84.28	93.41	85.38	93.41	84.67	93.41
Lungs	84.76	93.33	83.61	93.33	83.69	93.33	83.51	93.37	84.50	93.33	83.85	93.34
Breast	82.27	91.21	80.83	91.21	80.71	91.21	80.49	91.24	81.93	91.21	81.16	91.22
Ovaries	15.13	10.80	14.38	10.80	12.99	10.80	13.91	10.83	14.73	10.80	15.48	10.78
Uterus	12.63	3.60	11.34	3.55	11.26	3.55	11.07	3.57	12.13	3.55	12.40	3.56
Leg bones	84.02	93.26	82.87	93.28	82.84	93.28	82.65	93.30	83.72	93.28	83.20	93.29
Rectum	80.03	90.06	77.30	90.07	79.29	90.07	78.86	90.40	78.81	90.06	79.94	90.07
Mandible and teeth	86.11	95.19	84.88	95.20	84.85	95.20	84.74	95.33	85.65	95.20	85.33	95.20

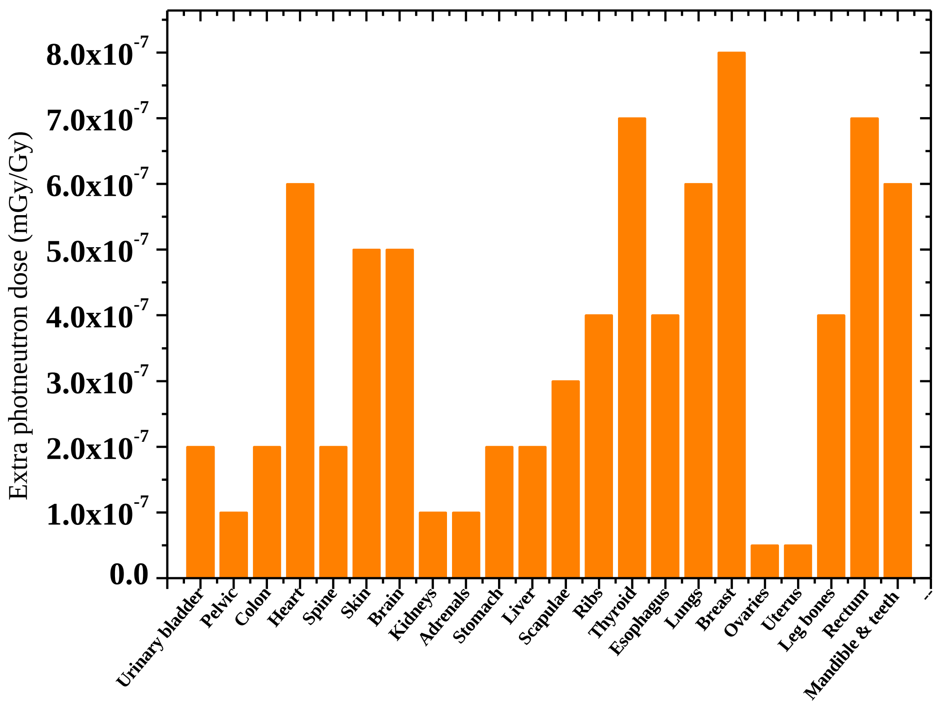

Figure 5. Extra photoneutron absorbed dose due to interaction of photon source with shield

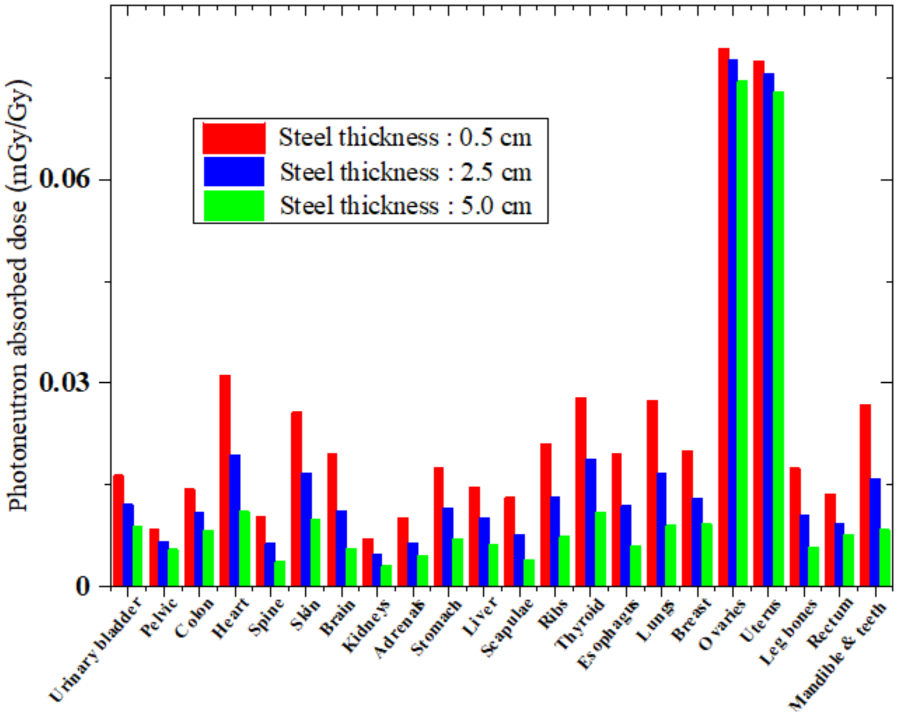

Figure 6. Photoneutron absorbed dose for different steel thicknesses in 15-MV linac

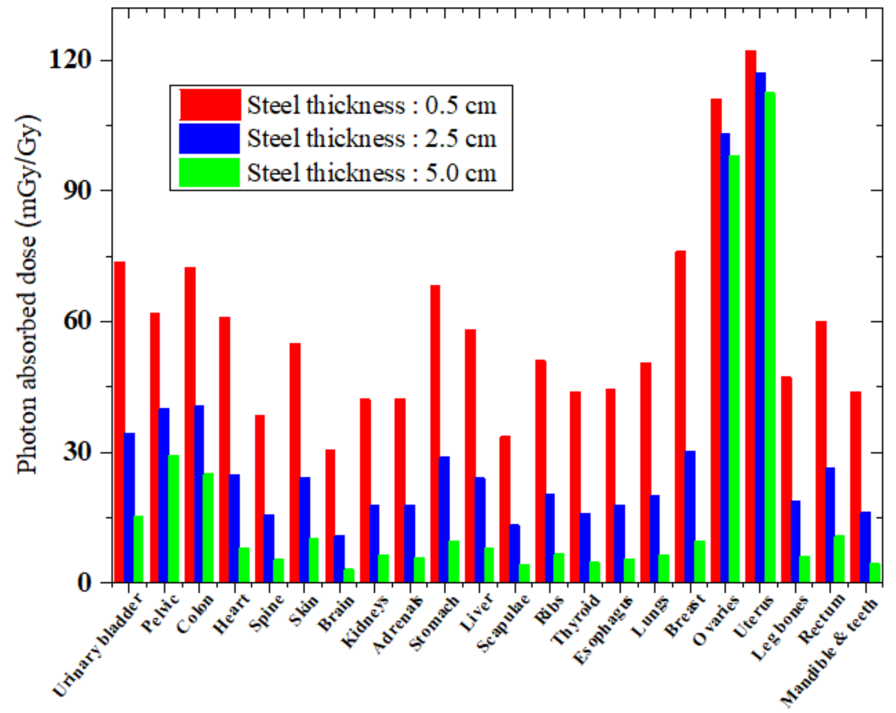

Figure 7. Photon absorbed dose for different steel thicknesses in 15-MV linac

Table 2. Range of photoneutron and photon reduction dose rates with various lengths of shield

Length of shield materials (cm)	Photoneutron dose reduction (%)	Photon dose reduction (%)
40	50-65	75-82
50	50-70	75-85
60	50-70	75-85
170	57-89	88-95

The obtained results showed that the smaller dimensions of the shield could also reduce a considerable amount of the photoneutron and photon in the phantom. Therefore, this shield may be applied even for each length with an arbitrary value of mass, along with the phantom.

Discussion

After analyzing the photon spectrum for linac 15 MV at the isocenter, a peak was observed near 0.3 MeV with a fluence of approximately 10^{-6} (cm^{-2}) and ending energy spectrum to the linac energy, in compliance with the findings of other studies [15, 16]. Figure 3 shows that the organs in the treatment field receive higher doses than others, and by increasing depth, the value of doses decreases. The results are in agreement with the findings of a study by Mohammadi et al. [8]. Furthermore, without shielding materials, the absorbed dose was within the range of 0.013-0.077 mGy/Gy due to radiation therapy, and the absorbed dose reduced considerably after using the shield.

It is observed that the photon absorbed dose was relatively high within the range of 75-118 mGy/Gy, and by the application of shielding structure, photon absorbed dose decreased significantly in the tissue and organ. The reduction rate, except for target volume, was reported within the range of 88-95%. Since steel thicknesses were twice as much thicker than the neutron absorbent, the photon reduction in the doses was greater than photoneutron reduction.

In line with the findings of studies performed by Sanchez-Doblado et al. and Roy et al. [6,13], the out-of-field photon absorbed dose is larger than the photoneutron absorbed dose, which due to their high biological effectiveness, photoneutrons harm healthy tissues more than photons.Photoneutron moderators were reported with similar behavior. By ignoring water containers during radiotherapy, all the materials can be used as a shield. Materials with less density in a definite volume are the best ones.

The range of reduction rate for photoneutron absorbed dose, presented in Table 1, is around 57-89%. As expected, the reduction rate in the target volume dose was not notable. The obtained results revealed that the extra photoneutron doses by photon source were nearly 10^5 times smaller than unwanted photoneutrons doses in neutron source, which can be ignored.

As it was observed in Figure 7, the value of the dose reduced by increasing the thickness of the steel. Since steel is a good photon absorbent, the reduction in a photon was remarkable. The reduction rate of doses was estimated in order to prove this fact. The obtained results revealed that for each 0.5 cm increase in steel thickness, photoneutron dose decreased by 6.5%, and the reduction rate for the photon was reported as 13%.

Weight and volume should be considered in spite of the premium attenuation and optimization of the shielding structure. Therefore, the maximum thickness of 5.0 cm for steel was investigated in this study. Consequently, the possibility to improve the proper shielding materials in order to reduce both photoneutron and photon doses, as well as ignorable extra photoneutron dose, was made available.

It is observed that the shorter length of the shield can also has a relatively performance for the reduction of unwanted doses in healthy tissues. Since the mass of a shield with a length of 40 cm is about 100 kg, it is necessary to design a suitable device, such as a wooden bridge [13, 17], to maintain and move the shielding structure.

Conclusion

In conclusion, out-of-field photoneutron and photon doses were estimated in the present study. Two models were simulated for photoneutron and photon sources for the calculation of the doses in organs and tissues in the presence of phantom and walls of the treatment room. According to ALARA, proper shielding structures were designed in order to optimize the dose. Therefore, neutron moderators, neutron absorbent, and gamma absorbent with the total thicknesses of 20 cm were applied as the shield throughout the phantom.

The reduction rate also showed that except for the target organ, the photoneutron and photon reduction rates in other tissues and organs were 57-89% and 88-95%, respectively. Extra photoneutron dose by photon source interaction with the shield was also ignorable. The thickness of steel as gamma absorbents was changed, and for each 0.5 cm increase in steel thickness, the reduction rates of photoneutron and photon doses were 6.5% and 13%, respectively. All neutron moderators had the same behavior; accordingly, the shield materials with less density in a definite volume were chosen in order to optimize the dose.

With the consideration of all previous results, it is feasible to design a unique shielding structure to reduce secondary doses to healthy organs or tissues and produce lower extra photoneutron dose due to shield for a 15-MV linac. The studied multilayer shield had relatively high mass and could not be used for moving and rotating without a properly designed structure for assembling; therefore, this problem may be one of the disadvantages of a multilayer system.

References

1. Thalhofer JL, Rebello WF, Correa SA, Silva AX, Souza EM, Batista DV. Calculation of dose in healthy organs, during radiotherapy 4-field box 3D conformal for prostate cancer, simulation of the Linac 2300, radiotherapy room and MAX phantom. 2013.
2. Kry SF, Salehpour M, Followill DS, Stovall M, Kuban DA, White RA, et al. Out-of-field photon and neutron dose equivalents from step-and-shoot intensity-modulated radiation therapy. International Journal of Radiation Oncology* Biology* Physics. 2005;62(4):1204-16. Doi: 10.1016/j.ijrobp.2004.12.091.

3. Martínez-Ovalle SA, Barquero R, Gómez-Ros JM, Lallena AM. Neutron dosimetry in organs of an adult human phantom using linacs with multileaf collimator in radiotherapy treatments. Medical physics. 2012;39(5):2854-66.
4. Ovalle SA. Neutron dose equivalent in tissue due to linacs of clinical use. Frontiers in Radiation Oncology. 2013;3: 91-112.
5. Khabaz R. Effect of each component of a LINAC therapy head on neutron and photon spectra. Applied Radiation and Isotopes. 2018; 139:40-5. Doi: 10.1016/j.apradiso.2018.04.022.
6. Sánchez-Doblado F, Domingo C, Gómez F, Sánchez-Nieto B, Muñiz JL, García-Fusté MJ, et al. Estimation of neutron-equivalent dose in organs of patients undergoing radiotherapy by the use of a novel online digital detector. Physics in Medicine & Biology. 2012;57(19):6167-91. Doi:10.1088/0031-9155/57/19/6167.
7. Kry SF, Howell RM, Salehpour M, Followill DS. Neutron spectra and dose equivalents calculated in tissue for high-energy radiation therapy. Medical physics. 2009;36(4):1244-50. Doi: 10.1118/1.3089810.
8. Mohammadi N, Miri-Hakimabad H, Rafat-Motavalli L, Akbari F, Abdollahi S. Patient-specific voxel phantom dosimetry during the prostate treatment with high-energy linac. Journal of Radioanalytical and Nuclear Chemistry. 2015;304(2):785-92. Doi: 10.1007/s10967-014-3872-9.
9. Khabaz R, Boodaghi R, Benam MR, Zanganeh V. Estimation of photoneutron dosimetric characteristics in tissues/organs using an improved simple model of linac head. Applied Radiation and Isotopes. 2018;133:88-94. Doi:10.1016/j.apradiso.2018.04.022.
10. NCRP. Neutron contamination from medical electron accelerators. NCRP Report No. 79. Bethesda, MD.1984.
11. ICRP. Recommendations of the international commission on radiological protection. ICRP Report No. 26. 1997.
12. Garrigó E, Zunino S, Germanier A. Protection of the contralateral breast during radiation therapy for breast cancer. 2008.
13. Roy SC, Sandison GA. Shielding for neutron scattered dose to the fetus in patients treated with 18 MV x-ray beams. Medical physics. 2000;27(8):1800-3. Doi:10.1118/1.1287438. Pub Med PMID: 10984226.
14. Khabaz R. Evaluation of an alternative convenient irradiation system for determination of emission rate of radio-isotopic neutron sources. Journal of Radioanalytical and Nuclear Chemistry. 2014;299(1):5-12. Doi: 10.1007/s 10967-013-2728-z.
15. Vega-Carrillo HR, Martinez-Ovalle SA, Lallena AM, Mercado GA, Benites-Rengifo JL. Neutron and photon spectra in LINACs. Applied Radiation and Isotopes. 2012;71:75-80. Doi: 10.1016/j.apradiso.2012.03.034.
16. Sheikh-Bagheri D, Rogers DW. Monte Carlo calculation of nine megavoltage photon beam spectra using the BEAM code. Medical physics. 2002;29(3):391-402. Doi: 10.1118/1.1445413.
17. Chu S. Shielding for radiation scattered dose distribution to the outside fields in patients treated with high energy radiotherapy beams. Proccedings of the International Conference on the Radiological Protection of Patients in Diagnostic and Interventional Radiology, Nuclear Medicine and Radiotherapy. Malaga, March; 2001.